Calibration Problem in Laser Ektacytometry of Erythrocytes

Sergey Y. Nikitin, Evgeniy G. Tsybrov*, and Mariia S. Lebedeva
M. V. Lomonosov Moscow State University, GSP-1 Leninskie Gory, Moscow 119991, Russia

*** e-mail:** tsybrovevgeniy@yandex.ru

Abstract. The problem of measuring the deformability of erythrocytes by laser diffractometry in shear flow (ektacytometry) is considered. The question of how the shape of the isointensity line in the diffraction pattern, which arises when a laser beam is scattered by an ensemble of erythrocytes, is related to the level of light intensity on this line, is analyzed. A simplified algorithm for measuring the parameters of the distribution of erythrocytes in deformability is proposed, which does not require photometry of the central part of the diffraction pattern. © 2022 Journal of Biomedical Photonics & Engineering.

Keywords: erythrocyte deformability; laser ektacytometry; data processing algorithms.

Paper #3541 received 22 Sep 2022; revised manuscript received 24 Oct 2022; accepted for publication 25 Oct 2022; published online 12 Dec 2022. doi: 10.18287/JBPE22.08.040503.

1 Introduction

One of the important rheological characteristics of blood is the deformability of erythrocytes, which is defined as a measure of the ability of these cells to change their shape under the action of external forces [1–5]. Measurement of this parameter is important in the diagnosis and treatment of sickle cell anemia [6], tropical malaria [7], hereditary spherocytosis [8], and many other diseases. The main methods for measuring the deformability of erythrocytes are presented in Refs. [9–13]. Various aspects of such measurements are discussed in Refs. [14–16]. The works [17–18] consider the factors affecting the deformability of erythrocytes and the possibilities of controlling this parameter.

Currently, one of the main methods for measuring the deformability of erythrocytes is laser diffractometry of erythrocytes in a shear flow (ektacytometry). Proposed in 1975 [19], this method was developed in Refs. [20–24]. The authors of works [25, 26] draw attention to the fact that it is important to be able to measure not only the average deformability of erythrocytes, but also the distribution of erythrocytes in deformability in the blood sample under study. In principle, such measurements can be performed by rheoscopy [27, 28]. However, this method is difficult to implement in practice.

In our works [29–34], we proposed algorithms for measuring the characteristics of the distribution of erythrocytes in deformability based on the method of laser ektacytometry. However, the problem of laser ektacytometer calibration, which consists in measuring the light intensity on the isointensity line of the diffraction pattern with respect to the intensity of the central diffraction maximum, remains on the way to the practical implementation of these algorithms. This problem is complicated by the fact that the center of the diffraction pattern is illuminated by a direct laser beam. Therefore, it is expedient to search for indirect calibration methods that do not require photometry of the diffraction pattern in its central part. One such method is proposed in this paper.

2 Laser Ektacytometry of Erythrocytes

In laser ektacytometry, a suspension of erythrocytes in a shear stress field is illuminated with a laser beam and a light scattering pattern (diffraction pattern) is observed. With an increase in shear stress, this pattern is extended in the direction perpendicular to the direction of shear flow, demonstrating the increasing deformation of erythrocytes under the influence of viscous friction forces.

The optical scheme of the laser ektacytometer is shown in Fig. 1. It includes a laser, a Couette cell into, which a highly diluted suspension of erythrocytes is poured, and an observation screen. Note that the diffraction pattern is located in that part of the observation screen where the direct laser beam radiation does not fall.

Examples of diffraction patterns obtained with a laser erythrocyte ektacytometer are shown in Fig. 2. Here, the pattern obtained at low shear stress is shown on the left, and the pattern obtained at high shear stress is shown on the right. The stretching of the diffraction pattern indicates the deformation of erythrocytes by the forces of viscous friction.

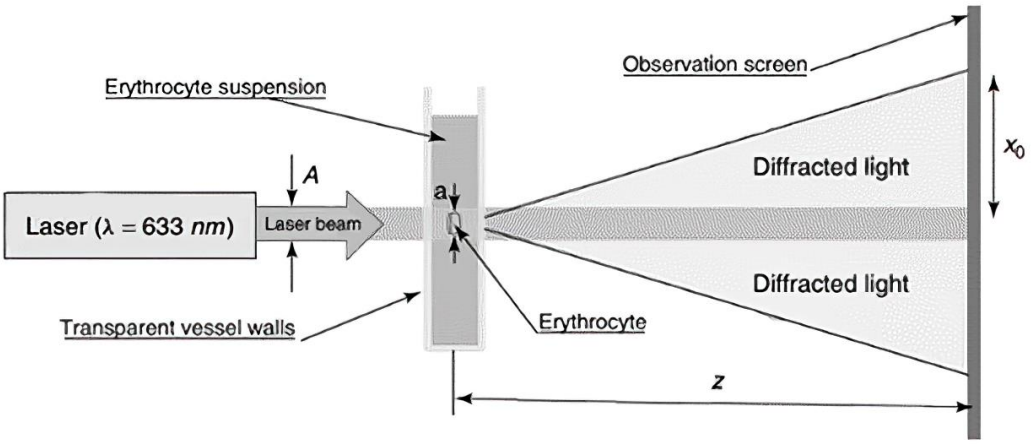

Fig. 1 Optical layout of a laser erythrocyte ektacytometer.

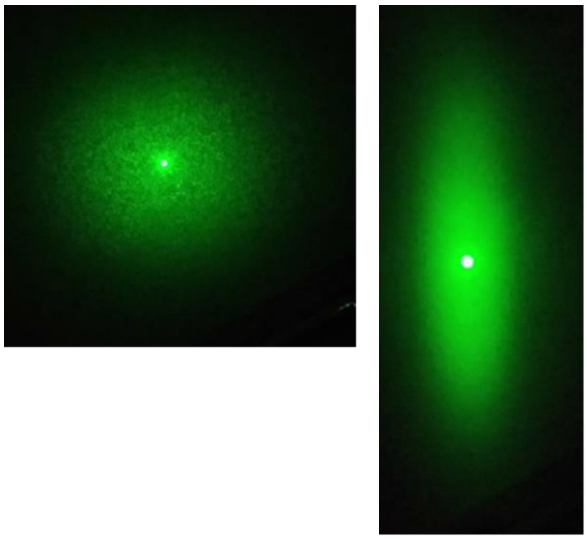

(a) (b)

Fig. 2 Examples of diffraction patterns obtained with a laser erythrocyte ectacytometer for a normal blood sample at low shear stress (a) and at high shear stress (b).

Existing laser erythrocyte ektacytometers, for example, LORRCA ektacytometer (Netherlands) [20], measure the geometrical parameter of the isointensity line – its aspect ratio – and on this basis determine the average deformability of erythrocytes s in the test blood sample. More advanced data processing algorithms make it possible to measure other parameters, in particular, the width μ, the asymmetry ν, and the kurtosis δ of the distribution of erythrocytes in deformability [29–34]. However, for this it is necessary to know not only the geometric parameters of the isointensity line, but also its energy parameter, which is equal to the ratio of the light intensity on this line to the intensity of the central diffraction maximum $\tilde{I} = I/I(0)$. In other words, it is necessary to calibrate the laser ektacytometer, which includes the task of photometry of the central part of the diffraction pattern. The importance of the parameter $\tilde{I}$ is due to the fact that the shape of the isointensity line depends on the level of light intensity on this line. This can be seen from Fig. 3, which shows three isointensity lines constructed for the same ensemble of erythrocytes, but differing in the level of light intensity. The analysis of the diffraction pattern is carried out on the basis of the concept of the isointensity line. This is the name of the set of points of the diffraction pattern, in which the light intensity has the same value $I = const$. An example of a diffraction pattern and isointensity line are shown in Fig. 4.

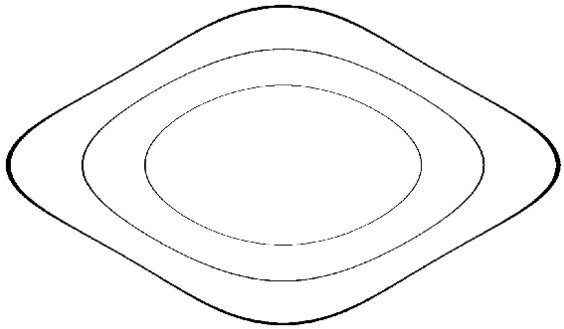

Fig. 3 Isointensity lines of the diffraction pattern corresponding to different levels of light intensity on the line (numerical simulation).

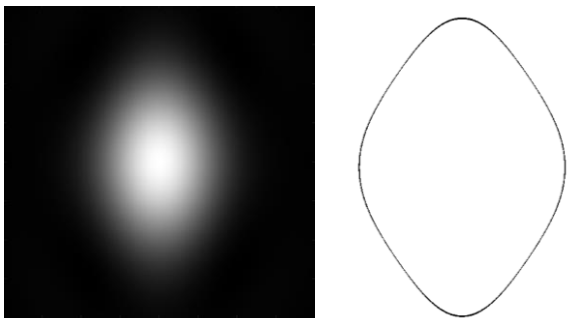

(a) (b)

Fig. 4 An example of a diffraction pattern (a) and an isointensity line (b).

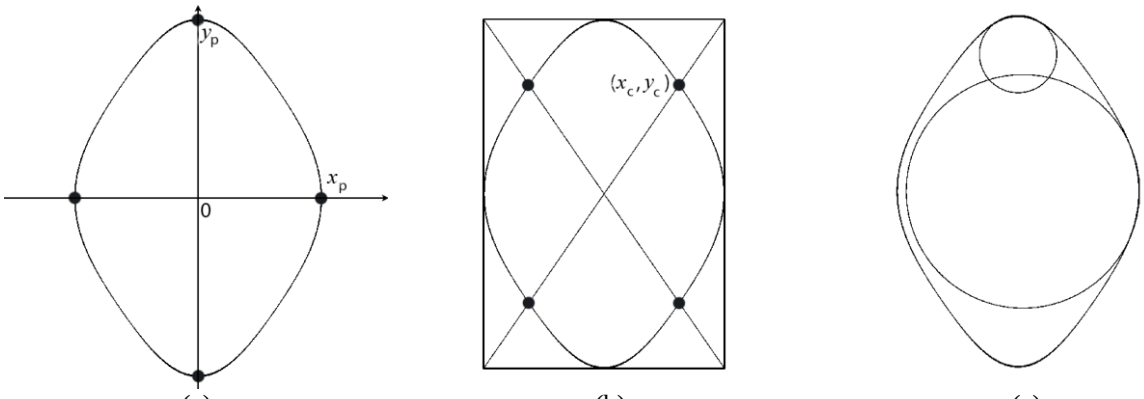

(a) (b) (c)

Fig. 5 Characteristics of the isointensity line of the diffraction pattern – polar points (a), characteristic points (b), circles of line curvature at polar points (c).

3 Isointensity Line and Its Geometric Parameters

Let us single out the polar and characteristic points of the isointensity line. Points lying on the symmetry axes of the isointensity line are called polar. Characteristic points are points lying on the diagonals of the rectangle enclosing this line. An example of an isointensity line, its polar and characteristic points are shown in Fig. 5.

Let us introduce a Cartesian coordinate system by placing the origin at the center of the diffraction pattern (the point of incidence of the direct laser beam on the observation screen) and directing the coordinate axes along the symmetry axes of the isointensity line. Let us denote the coordinates of the polar points x_p, y_p, the coordinates of the characteristic point x_c, y_c. Then $x_c / x_p = y_c / y_p$. We also introduce the radii of curvature of the isointensity line at the polar points, denoting them $R(x_p)$ and $R(y_p)$.

Algorithms for processing laser ectacytometry data are based on solving the problem of laser beam scattering by an ensemble of erythrocytes. An analytical solution of this problem is possible on the basis of a number of approximations. These include the approximation of single light scattering by erythrocytes, the approximation of anomalous diffraction, the approximation of small-angle scattering, the approximation of the far zone of diffraction, the approximation of weak inhomogeneity of the ensemble of erythrocytes. In addition, we restrict the calculation to the peripheral part of the diffraction pattern, in which the light intensities are approximately an order of magnitude lower than the intensity of the central diffraction maximum. As the analysis shows, it is this part of the diffraction pattern that is most sensitive to the parameters of the erythrocyte ensemble. As a result, it is possible to obtain approximate analytical relationships between the parameters of the isointensity line (x_p, y_p, x_c, y_c, $R(x_p)$, $R(y_p)$, $\tilde{I}$) and the characteristics of the erythrocyte ensemble of interest to us (s, μ, ν) – diffractometric equations. By solving these equations, we construct data processing algorithms. In this paper, we consider two such algorithms, the characteristic point algorithm [31] and the line curvature algorithm [33].

4 Characteristic Point Algorithm

The characteristic point algorithm [31] is applicable to ensembles of erythrocytes with a symmetric deformability distribution function. This algorithm is expressed by the formulas:

$$\begin{aligned} s &= D; \\ \mu_p &= \frac{2(1-Q)}{5+(F_0-1)Q}. \end{aligned} \tag{1}$$

Here

$$\begin{aligned} D &= \frac{y_p}{x_p}; \\ Q &= \frac{1}{\sqrt{2}}\left(\frac{x_c}{x_p}+\frac{y_c}{y_p}\right). \end{aligned} \tag{2}$$

$$\begin{aligned} F_0 &= \frac{1}{\sqrt{f_0}}; \\ f_0 &= \frac{1}{4\beta^2}\cdot\tilde{I}; \\ \beta &= -0.4. \end{aligned} \tag{3}$$

5 Line Curvature Algorithm

The line curvature algorithm [33] is applicable to erythrocyte ensembles with an arbitrary deformability distribution function. This algorithm gives the expression for μ as

$$\mu = \frac{1}{2q_1}\cdot\left(\frac{C_2}{s}+C_1 s\right)-\frac{1}{q_1},$$

where

$$\begin{aligned} C_1 &= \sqrt{\frac{x_p}{R(x_p)}}; \\ C_2 &= \sqrt{\frac{y_p}{R(y_p)}}; \\ q_1 &= 2(4+F_0). \end{aligned} \tag{4}$$

In particular, for an ensemble of erythrocytes with a symmetric deformability distribution function, when $\nu = 0$ and $s = D$, we obtain

$$\mu_l = \frac{C}{4(4+F_0)}, \quad (5)$$

where

$$C = \frac{C_2}{D} + C_1 D - 2. \quad (6)$$

6 Calibration Equation

Using Eqs. (1) and (5) and assuming $\mu_p = \mu_l$, we obtain an equation for F_0, from which it follows that

$$F_{0c} = \frac{32(1-Q)+(Q-5)C}{QC-8(1-Q)}. \quad (7)$$

This Eq., applicable to ensembles of erythrocytes with a symmetrical distribution in deformability, expresses the energy parameter of the isointensity line F_0 (3) through the geometric parameters of this line Q and C. These parameters are defined by Eqs. (2), (4), and (6). We will define Eq. (7) as the calibration equation. The result obtained can be formulated as follows: if the distribution of erythrocytes in deformability is symmetrical ("symmetric ensemble"), then the relative light intensity on the isointensity line is determined by its geometric parameters.

7 Symmetrical Ensemble of Erythrocytes and a Combined Algorithm for Measuring the Parameters of the Distribution of Erythrocytes in Deformability

Based on Eqs. (1) and (7), we can propose a new algorithm for measuring the width of the distribution of erythrocytes in deformability, which we entitiled the combined algorithm. This algorithm is applicable to ensembles of erythrocytes with a symmetric deformability distribution function and is expressed by the formula

$$\mu_c = \frac{2}{5} - \frac{Q \cdot C}{20(1-Q)}. \quad (8)$$

Here the parameters Q and C are defined by Eqs. (2), (4), and (6). As can be seen from these Eqs., the combined algorithm does not require the measurement of the relative light intensity (parameter $\check{I}$) on the isointensity line chosen for measurements. As input data, only the geometric parameters of the isointensity line are needed: $x_p, y_p, x_c, y_c, R(x_p), R(y_p)$. These parameters are the coordinates of the polar and characteristic points, as well as the radii of curvature of the line at the polar points.

8 Symmetry Criterion for an Ensemble of Erythrocytes

As for the condition of applicability of the combined algorithm related to the symmetry of the distribution of erythrocytes in deformability, this condition will be satisfied if $D = s = const$, i.e. if the aspect ratio of the isointensity line (parameter D) does not depend on the relative intensity of light on this line (parameter $\check{I}$). An example of such a situation is shown in the Fig. 6, which shows two close isointensity lines of the diffraction pattern with the same aspect ratios.

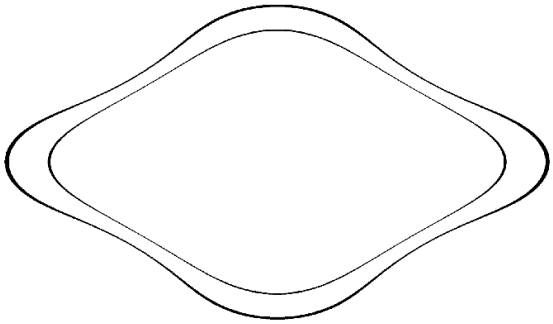

Fig. 6 Two close isointensity lines of the diffraction pattern, constructed for a symmetrical ensemble of erythrocytes (numerical simulation).

9 Verification of the Algorithm in a Numerical Experiment

A numerical experiment can be used to test the combined algorithm and evaluate its accuracy and range of applicability both in relation to the allowable inhomogeneity of the ensemble of erythrocytes and in relation to the part of the diffraction pattern suitable for measurements. We will do this using the example of a bimodal ensemble of erythrocytes, in which there are only two types of cells – soft (deformable) and hard (non-deformable) erythrocytes. The aspect ratios of cells in the shear flow of the laser ektacytometer will be denoted as s_1 (hard cells) and s_2 (soft cells). Let us put $s_1 = 1$ and we will change the parameter s_2 in a certain interval, thus modeling ensembles of erythrocytes with differences in the degree of heterogeneity. In all cases, we will assume the proportions of cells of both types in the blood sample to be the same $p = 1/2$, which corresponds to the model of a symmetrical ensemble of erythrocytes.

The normalized distribution of light intensity in the diffraction pattern is described by the Eq. [31]:

$$\check{I}(x,y) = \frac{(a_1 b_1)^2 G\left(\frac{k}{z}\sqrt{a_1^2 x^2 + b_1^2 y^2}\right) + (a_2 b_2)^2 G\left(\frac{k}{z}\sqrt{a_2^2 x^2 + b_2^2 y^2}\right)}{(a_1 b_1)^2 + (a_2 b_2)^2}. \quad (9)$$

Here x, y are the Cartesian coordinates of a point on the observation screen, z is the distance from the measuring volume to the observation screen, $k = 2\pi/\lambda$ is the

wavenumber, λ is the laser wavelength. The remaining parameters are expressed by the following Eqs.:

$$a_1 = a_0 \cdot (1 + \varepsilon_1); \quad b_1 = b_0 \cdot (1 - \varepsilon_1). \tag{10}$$

$$a_2 = a_0 \cdot (1 + \varepsilon_2); \quad b_2 = b_0 \cdot (1 - \varepsilon_2). \tag{11}$$

$$s = \sqrt{s_2}; \quad \varepsilon_1 = \frac{s_1 - s}{s_1 + s}; \quad \varepsilon_2 = \frac{s_2 - s}{s_2 + s}; \quad b_0 = a_0/s. \tag{12}$$

In this case, the exact value of the parameter μ as

$$\mu = \frac{1}{2}(\varepsilon_1^2 + \varepsilon_2^2). \tag{13}$$

The function $G(x)$ is defined by a following Eq.:

$$G(x) = [2J_1(x)/x]^2, \tag{14}$$

where $J_1(x)$ is the first order Bessel function. In the calculations, we assumed $a_0 = 7\ \mu m$, $\lambda = 0.65\ \mu m$, and $z = 10^6\ \mu m$. The verification procedure is as follows. Assuming $\tilde{I} = const$ and choosing the value of the parameter $\tilde{I}$, by Eqs. (9–12) and (14), we construct the isointensity line of the diffraction pattern, which is described by the function $y = y(x)$ or $x = x(y)$. We find the coordinates of the polar and characteristic points of this line, shown in Fig. 4, determine the aspect ratio of the line D and calculate the parameter Q by Eq. (2).

In a real experiment, the parameters of the curvature of the isointensity line can be calculated using Eq. (4). In the particular case of a bimodal ensemble of erythrocytes, these parameters can be calculated analytically using the formulas obtained in Ref. [33]. Let us use these formulas here. First, we find the normalized coordinates of the polar points U_p and V_p solving transcendental equations

$$\tilde{I} = \frac{(1-\varepsilon_1^2)^2 \cdot G[(1+\varepsilon_1)U_p] + (1-\varepsilon_2^2)^2 \cdot G[(1+\varepsilon_2)U_p]}{(1-\varepsilon_1^2)^2 + (1-\varepsilon_2^2)^2}; \tag{15}$$

$$\tilde{I} = \frac{(1-\varepsilon_1^2)^2 \cdot G[(1-\varepsilon_1)V_p] + (1-\varepsilon_2^2)^2 \cdot G[(1-\varepsilon_2)V_p]}{(1-\varepsilon_1^2)^2 + (1-\varepsilon_2^2)^2}. \tag{16}$$

Then we calculate the parameters of the curvature of the isointensity line using the following Eqs.:

$$C_1 = \frac{1}{s}\sqrt{\frac{g_{1U}G'[(1+\varepsilon_1)U_p] + g_{2U}G'[(1+\varepsilon_2)U_p]}{h_{1U}G'[(1+\varepsilon_1)U_p] + h_{2U}G'[(1+\varepsilon_2)U_p]}}; \tag{17}$$

$$C_2 = s\sqrt{\frac{g_{1V}G'[(1-\varepsilon_1)V_p] + g_{2V}G'[(1-\varepsilon_2)V_p]}{h_{1V}G'[(1-\varepsilon_1)V_p] + h_{2V}G'[(1-\varepsilon_2)V_p]}}. \tag{18}$$

Here

$$g_{1U} = \frac{1}{2}(1-\varepsilon_1)^4(1+\varepsilon_1); \quad g_{2U} = \frac{1}{2}(1-\varepsilon_2)^4(1+\varepsilon_2); \tag{19}$$

$$h_{1U} = \frac{1}{2}(1-\varepsilon_1)^2(1+\varepsilon_1)^3; \quad h_{2U} = \frac{1}{2}(1-\varepsilon_2)^2(1+\varepsilon_2)^3; \tag{20}$$

$$g_{1V} = \frac{1}{2}(1-\varepsilon_1)(1+\varepsilon_1)^4; \quad g_{2V} = \frac{1}{2}(1-\varepsilon_2)(1+\varepsilon_2)^4; \tag{21}$$

$$h_{1V} = \frac{1}{2}(1-\varepsilon_1)^3(1+\varepsilon_1)^2; \quad h_{2V} = \frac{1}{2}(1-\varepsilon_2)^3(1+\varepsilon_2)^2 \tag{22}$$

and the function $G'(x)$ is defined by the Eq. (23):

$$G'(x) = \frac{8}{x^3} \cdot [xJ_0(x) - 2J_1(x)]J_1(x), \tag{23}$$

where $J_0(x)$ is the zero order Bessel function.

10 Results and Discussion

Let us consider a numerical example. Let us set s_2 = 2.1 and $\tilde{I}$ = 0.053. The diffraction pattern and the isointensity line with such parameters are shown in Fig. 4, 5. Making calculations according to Eqs. (1–3) and (5–23), we obtain s = 1.45, μ = 0.0336, D = 1.45, Q = 0.885, C = 0.953, F_0 = 3.47, F_{0c} = 3.28, μ_p = 0.0319, μ_l = 0.0319, and μ_c = 0.0327.

Here, all values are rounded to the nearest three significant figures. It can be seen that in this case, the measurement error of the F_0 parameter using the calibration Eq. (7) is 5%, the measurement error of the parameter μ using the characteristic point algorithm, Eq. (1), and the line curvature algorithm Eq. (5) is 5%, the measurement error of the parameter μ using combined algorithm Eq. (8) is 3%. Thus, with the correct choice of the isointensity line, the accuracy of all algorithms turns out to be quite high. More complete data is given in the Figs. 7 and 8.

In practice, to assess the heterogeneity of the ensemble of erythrocytes in terms of deformability, it is convenient to use the parameter $\mu' = \sqrt{\mu}$. This parameter has the meaning of a standard deviation or a measure of the scatter of erythrocytes in deformability in the test blood sample and can be expressed as a percentage.

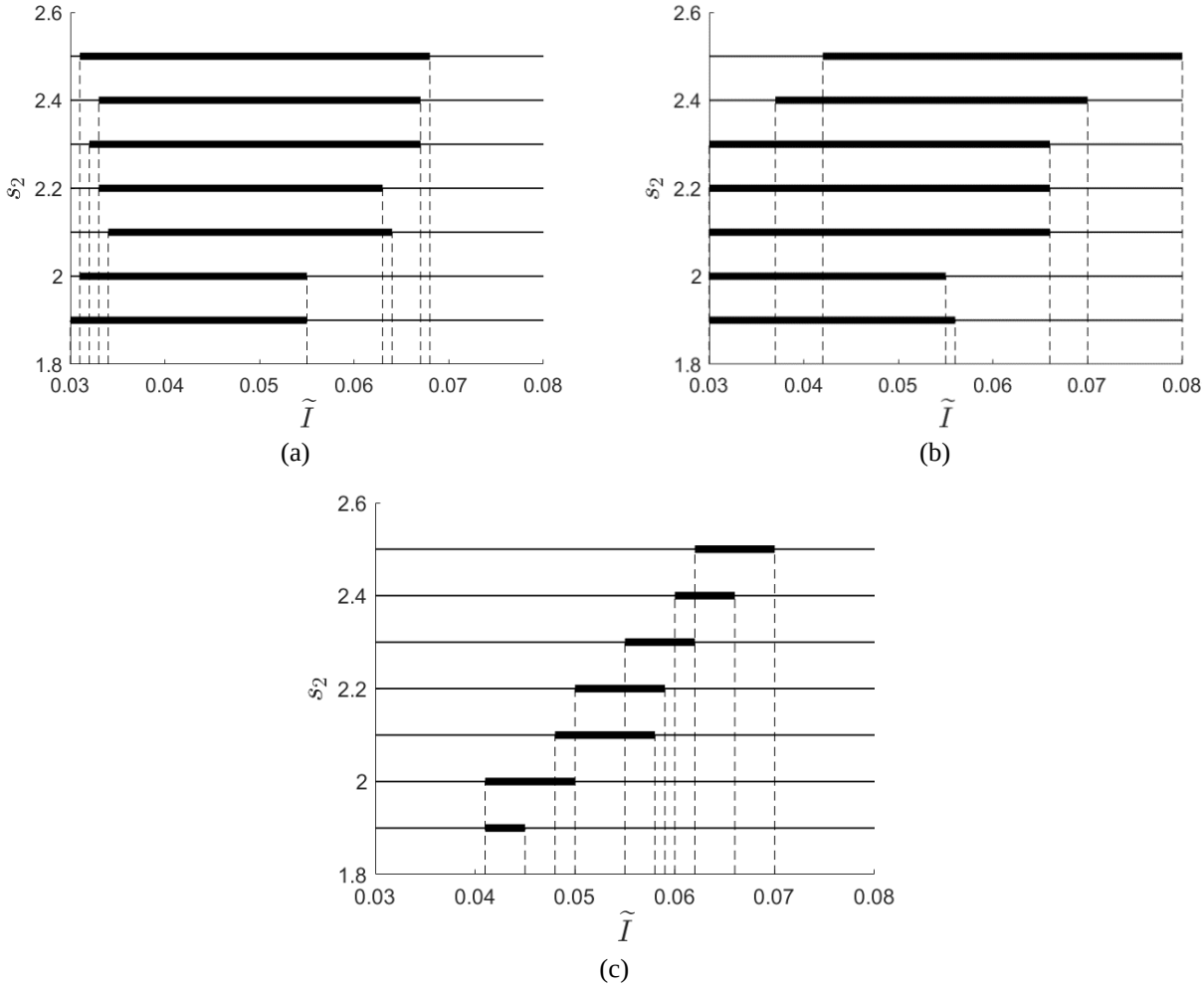

Fig. 7 Scope of applicability of the algorithms. The abscissa shows the normalized light intensity on the isointensity line chosen for measurements. The ordinate shows the aspect ratio of the soft (deformable) component of the erythrocyte ensemble in the shear flow of the laser ektacytometer. Bold horizontal lines show areas for which the measurement error of the parameter μ (erythrocyte deformability dispersion) does not exceed 10% using: (a) the characteristic point algorithm Eq. (1); (b) the line curvature algorithm Eq. (5); (c) the combined algorithm Eq. (8).

Table 1 Estimation of the Accuracy of the Combined Algorithm for Measuring the Deformability Spread of Erythrocytes (Numerical Experiment).

s_2	$\tilde{I}$	μ	μ′(%)	μ_c	μ_c' (%)	δμ′(%)
1.9	0.041	0.0253	15.9	0.0245	15.6	1.9
1.9	0.043	0.0253	15.9	0.0242	15.6	1.9
1.9	0.045	0.0253	15.9	0.0241	15.5	2.5
2.1	0.048	0.0336	18.3	0.0358	18.9	3.2
2.1	0.052	0.0336	18.3	0.0335	18.3	0
2.1	0.056	0.0336	18.3	0.0307	17.5	4.4
2.3	0.055	0.0422	20.5	0.0448	21.2	3.4
2.3	0.058	0.0422	20.5	0.0420	20.5	0
2.3	0.062	0.0422	20.5	0.0386	19.6	4.4
2.5	0.062	0.0507	22.5	0.0555	23.6	4.9
2.5	0.066	0.0507	22.5	0.0520	22.8	1.3
2.5	0.070	0.0507	22.5	0.0466	21.6	4.0

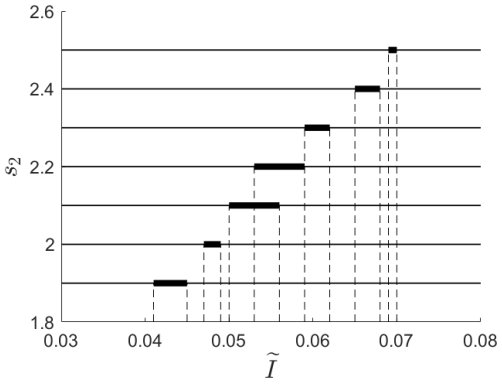

Fig. 8 Range of applicability of the calibration equation. The abscissa shows the normalized light intensity on the isointensity line chosen for measurements. The ordinate shows the aspect ratio of the soft (deformable) component of the erythrocyte ensemble in the shear flow of the laser ektacytometer. Bold horizontal lines show areas for which the measurement error of the parameter F_0 using the calibration equation (7) does not exceed 10%.

Using a combined algorithm, a parameter $\mu_c' = \sqrt{\mu_c}$ can be measured. Data on the accuracy and range of applicability of the combined algorithm are presented in Table 1. This table shows the values of the parameters s_2, $\tilde{I}$, μ, μ′, μ_c, μ_c', as well as the parameter $\delta\mu' = \frac{|\mu' - \mu_c'|}{\mu'} \cdot 100\%$, which has the meaning of the error in measuring the spread of erythrocytes in deformability using the combined algorithm Eq. (8). The values of all quantities are given with an accuracy of three significant figures. It can be seen that in all considered cases the error of the combined algorithm does not exceed 5%. In this case, the scatter of erythrocytes in deformability varies from 15.9% to 22.5%, and the relative light intensity on the isointensity line chosen for measurements lies in the range from 0.04 to 0.07. We note once again that the input data for this algorithm are only the geometric parameters of the isointensity line chosen for measurements, and it is not required to determine the level of light intensity on this line. This eliminates the need to photometer the central part of the diffraction pattern, which greatly simplifies the measurement procedure in laser ektacytometry of erythrocytes.

11 Conclusion

In this paper, we consider the problem of measuring the deformability of erythrocytes by laser diffractometry in shear flow (ektacytometry). The question of how the shape of the isointensity line in the diffraction pattern, which arises when a laser beam is scattered by an ensemble of erythrocytes, is related to the level of light intensity on this line, is analyzed. It is shown that if the distribution of erythrocytes in deformability is symmetrical ("symmetrical ensemble"), then the relative level of light intensity on the isointensity line is determined by its geometric parameters. The ensemble symmetry criterion is that the aspect ratio of the isointensity line does not depend on the level of light intensity on this line. An equation is obtained that expresses the relative intensity of light on the isointensity line in terms of its geometric parameters (calibration equation). Based on the calibration equation, a new algorithm for processing erythrocyte laser ectacytometry data (combined algorithm) is proposed, the input data for which are only the geometric parameters of the diffraction pattern that occurs when a laser beam is scattered by an ensemble of erythrocytes in a laser ektacytometer. The algorithm is designed to measure the spread of erythrocytes in deformability in the test blood sample under conditions when the distribution function of erythrocytes in terms of deformability is symmetrical. Using the numerical simulation method, we evaluated the accuracy of the combined algorithm and the area of its applicability both in relation to the allowable inhomogeneity of the ensemble of erythrocytes and the part of the diffraction pattern suitable for measurements. Numerical calculations performed for heterogeneous ensembles of erythrocytes, with a spread in deformability from 15% to 22%, showed that with an appropriate choice of the isointensity line in the diffraction pattern, the width of the distribution of erythrocytes in deformability can be measured using the combined algorithm with an error not exceeding 5%. In this case, the light intensity on the isointensity line with respect to the central maximum of the diffraction pattern is from 4% to 7%. The data obtained can be used to measure the scatter of erythrocytes in deformability by laser ektacytometry under conditions where only the peripheral part of the diffraction pattern is available for observation, and direct calibration of the laser ektacytometer is difficult.

Disclosures

The authors declare no conflict of interest.

Acknowledgments

The authors are grateful to A. V. Priezzhev, A. E. Lugovtsov, and V. D. Ustinov for their interest in the work and useful discussions. The work was carried out within the framework of the Development Program of the Interdisciplinary Scientific and Educational School of Moscow University "Photonic and Quantum Technologies. Digital Medicine" and with the financial support of the RSF grant No. 22-15-00120.

References

1. F. C. Mokken, M. Kedaria, Ch. P. Henny, M. R. Hardeman, and A. W. Gelb, "The clinical importance of erythrocyte deformability, a hemorrheological parameter," Annals of Hematology 64(3), 113–122 (1992).
2. S. Shin, Y. Ku, M.-S. Park, and J.-S. Suh, "Deformability of Red Blood Cells: A Determinant of Blood Viscosity," Journal of Mechanical Science and Technology 19(1), 216–223 (2005).
3. K. Toth, G. Kesmarky, and T. Alexy, "Clinical significance of hemorheological alterations," in Handbook of Hemorheology and Hemodynamics, O. K. Baskurt, M. R. Hardeman, M. W. Rampling, and H. J. Meiselman (Eds.), IOS Press, Amsterdam, Netherlands (2007). ISBN: 978-1-58603-771-0.
4. R. Huisjes, A. Bogdanova, W. W. van Solinge, R. M. Schiffelers, L. Kaestner, and R. van Wijk, "Squeezing for Life - Properties of Red Blood Cell Deformability," Frontiers in Physiology 9, 656 (2018).
5. E. Nader, S. Skinner, M. Romana, R. Fort, N. Lemonne, N. Guillot, A. Gauthier, S. Antoine-Jonville, C. Renoux, M.-D. Hardy-Dessources, E. Stauffer, P. Joly, Y. Bertrand, and P. Connes, "Blood Rheology: Key Parameters, Impact on Blood Flow, Role in Sickle Cell Disease and Effects of Exercise," Frontiers in Physiology 10, 1329 (2019).
6. M. Rabai, J. A. Detterich, R. B. Wenby, T. M. Hernandez, K. Toth, H. J. Meiselman, and J. C. Wood, "Deformability analysis of sickle blood using ektacytometry," Biorheology 51(2–3), 159–170 (2014).
7. A. M. Dondorp, B. J. Angus, M. R. Hardeman, K. T. Chotivanich, K. Silamut, R. Ruangveerayuth, P. A. Kager, N. J. White, and J. Vreeken, "Prognostic significance of reduced red blood cell deformability in severe falciparum malaria," American Society of Tropical Medicine and Hygiene 57(5), 507–511 (1997).
8. L. Da Costa, J. Galimand, O. Fenneteau, and N. Mohandas, "Hereditary spherocytosis, elliptocytosis, and other red cell membrane disorders," Blood Reviews 27(4), 167–178 (2013).
9. M. Musielak, "Red blood cell-deformability measurement: Review of techniques," Clinical Hemorheology and Microcirculation 42, 47–64 (2009).
10. O. K. Baskurt, M. Boynard, G. C. Cokelet, P. Connes, B. M. Cooke, S. Forconi, F. Liao, M. R. Hardeman, F. Jung, H. J. Meiselman, G. Nash, N. Nemeth, B. Neu, B. Sandhagen, S. Shin, G. Thurston, and J. L. Wautier, "New guidelines for hemorheological laboratory techniques," Clinical Hemorheology and Microcirculation 42(2), 75–97 (2009).
11. Y. Kim, K. Kim, and Y. Keun, "Measurement Techniques for Red Blood Cell Deformability: Recent Advances," Chapter 10 in Blood Cell – An Overview of Studies in Hematology, T. E. Moschandreou (Ed.), InTechOpen, Rijeka, Croatia (2012). ISBN: 978-953-51-0753-8.
12. J. Kim, H. Lee, and S. Shin, "Advances in the measurement of red blood cell deformability: A brief review," Journal of Cellular Biotechnology 1(1), 63–79 (2015).
13. C. Saldanha, "Instrumental analysis applied to erythrocyte properties," Journal of Cellular Biotechnology 1(1), 81–93 (2015).
14. Q. Guo, S. P. Duffy, K. Matthews, A. T. Santoso, M. D. Scott, and H. Ma, "Microfluidic analysis of red blood cell deformability," Journal of Biomechanics 47, 1767–1776 (2014).
15. E. S. Lamoureux, E. Islamzada, M. V. J. Wiens, K. Matthews, S. P. Duffy, and H. Ma, "Assessing red blood cell deformability from microscopy images using deep learning," Lab on a Chip 22(1), 26–39 (2021).
16. A. Finkelstein, H. Talbot, S. Topsu, T. Cynober, L. Garçon, G. Havkin, and F. Kuypers, "Comparison between a Camera and a Four Quadrant Detector, in the Measurement of Red Blood Cell Deformability as a Function of Osmolality," Journal of Medical and Bioengineering 2(1), 62–65 (2013).
17. A. V. Muravyov, I. A. Tikhomirova, "Role molecular signaling pathways in changes of red blood cell deformability," Clinical Hemorheology and Microcirculation 53, 45–59 (2013).
18. A. N. Semenov, E. A. Shirshin, A. V. Muravyov, and A. V. Priezzhev, "The Effects of Different Signaling Pathways in Adenylyl Cyclase Stimulation on Red Blood Cells Deformability," Frontiers in Physiology 10, 923 (2019).
19. M. Bessis, N. Mohandas, "A diffractometric method for the measurement of cellular deformability," Blood Cells 1, 307–313 (1975).
20. M. R. Hardeman, P. T. Goedhart, J. G. G. Dobbe, and K. P. Lettinga, "Laser-assisted Optical Rotational Analyser (LORCA); I. A new instrument for measurement of various structural hemorheological parameters," Clinical Hemorheology and Microcirculation 14(4), 605–618 (1994).
21. S. Shin, Y. Ku, M.-S. Park, and J.-S. Suh, "Slit-Flow Ektacytometry: Laser Diffraction in a Slit Rheometer," Cytometry Part B: Clinical Cytometry: The Journal of the International Society for Analytical Cytology 65B(1), 6–13 (2005).
22. S. Shin, Y. Ku, M.-S. Park, J.-H. Jang, and J.-S. Suh, "Rapid cell-deformability sensing system based on slit-flow laser diffractometry with decreasing pressure differential," Biosensors and Bioelectronics 20(7), 1291–1297 (2005).
23. M. A. E. Rab, B. A. van Oirschot, J. Bos, T. H. Merkx, A. C. W. van Wesel, O. Abdulmalik, M. K. Safo, B. A. Versluijs, M. E. Houwing, M. H. Cnossen, J. Riedl, R. E. G. Schutgens, G. Pasterkamp, M. Bartels, E. J. van Beers, and R. van Wijk, "Rapid and reproducible characterization of sickling during automated deoxygenation in sickle cell disease patients," American Journal of Hematology 94(5), 575–584 (2019).

24. O. K. Baskurt, M. R. Hardeman, M. Uyuklu, P. Ulker, M. Cengiz, N. Nemeth, S. Shin, T. Alexy, and H. J. Meiselman, "Comparison of three commercially available ektacytometers with different shearing geometries," Biorheology 46(3), 251–264 (2009).
25. N. L. Parrow, P.-C. Violet, H. Tu, J. Nichols, C. A. Pittman, C. Fitzhugh, R. E. Fleming, N. Mohandas, J. F. Tisdale, and M. Levine, "Measuring Deformability and Red Cell Heterogeneity in Blood by Ektacytometry," Journal of Visualized Experiments 131, e56910 (2018).
26. C. Renoux, N. Parrow, C. Faes, P. Joly, M. Hardeman, J. Tisdale, M. Levine, N. Garnier, Y. Bertrand, K. Kebaili, D. Cuzzubbo, G. Cannas, C. Martin, and P. Connes, "Importance of methodological standardization for the ektacytometric measures of red blood cell deformability in sickle cell anemia," Clinical Hemorheology and Microcirculation 62(2), 173–179 (2016).
27. J. G. G. Dobbe, M. R. Hardeman, G. J. Streekstra, J. Starckee, C. Ince, and C. A. Grimbergen, "Analyzing red blood cell-deformability distributions," Blood Cells, Molecules, and Diseases 28(3), 373–384 (2002).
28. J. G. G. Dobbe, G. J. Streekstra, M. R. Hardeman, C. Ince, and C. A. Grimbergen, "Measurement of the Distribution of Red Blood Cell Deformability Using an Automated Rheoscope," Cytometry: The Journal of the International Society for Analytical Cytology 50(6), 313–325 (2002).
29. S. Yu. Nikitin, A. V. Priezzhev, A. E. Lugovtsov, V. D. Ustinov, and A. V. Razgulin, "Laser ektacytometry and evaluation of statistical characteristics of inhomogeneous ensembles of red blood cells," Journal of Quantitative Spectroscopy and Radiative Transfer 146, 365–375 (2014).
30. S. Yu. Nikitin, A. E. Lugovtsov, V. D. Ustinov, M. D. Lin, and A. V. Priezzhev, "Study of laser beam scattering by inhomogeneous ensemble of red blood cells in a shear flow," Journal of Innovative Optical Health Science 8(4), 1550031 (2015).
31. S. Yu. Nikitin, V. D. Ustinov, "Characteristic point algorithm in laser ektacytometry of red blood cells," Quantum Electronics 48(1), 70–74 (2018).
32. S. Yu. Nikitin, "On the possibility of measuring the excess coefficient of the erythrocyte deformability distribution by laser ektacytometry," Quantum Electronics 48(10), 983–987 (2018).
33. S. Yu. Nikitin, V. D. Ustinov, S. D. Shishkin, and M. S. Lebedeva, "Line curvature algorithm in laser ektacytometry of red blood cells," Quantum Electronics 50(9), 888–894 (2020).
34. S. Yu. Nikitin, V. D. Ustinov, and S. D. Shishkin, "Band point algorithms for measuring diffraction pattern parameters in laser ektacytometry of red blood cell," Quantum Electronics 51(4), 353–358 (2021).